Tribology International 114 (2017) 201–207

Contents lists available at ScienceDirect

Tribology International

journal homepage: www.elsevier.com/locate/triboint

Frictional behaviour and friction mechanisms of rolling-sliding contact in mixed EHL

Xiaogang Zhang[a,*], Sangarapillai Kanapathipillai[a], Tonghai Wu[b], Zhongxiao Peng[a]

[a] School of Mechanical and Manufacturing Engineering, UNSW Australia, Sydney, NSW 2052, Australia
[b] Theory of Lubrication and Bearing Institute, Xi'an Jiaotong University, Xian 710049, China

ARTICLE INFO

Keywords:
Friction coefficient
Mixed EHL
Boundary film
Solid-to-solid friction

ABSTRACT

Frictional behaviour of mixed Elasto-hydrodynamic lubrication (EHL) arises from the coupling of the lubricant fluid and asperity interaction frictions. Due to the difficulties in modelling asperity interaction friction, existing approaches often use a constant friction coefficient obtained in boundary lubrication to approach the asperity interaction friction coefficient in mixed EHL. In this study, the asperity interaction friction is, for the first time, considered to result from either the boundary film friction or solid-to-solid ploughing and adhesion friction depending on the local contact and deformation conditions. The friction of mixed EHL was predicted by the combination result of lubricants fluid, boundary film, and solid-to-solid frictions. This development provides an alternative and cost effective method to estimate friction coefficient in mixed EHL.

1. Introduction

Rolling-sliding contacts widely exist in mechanical components, such as gears and roller bearings. The prediction of their frictional behaviour is of importance for several purposes, including friction reduction, energy conservation, and improving service life. For a properly lubricated rolling-sliding contact, the surfaces are often separated by lubricants, and the applied load is carried by hydrodynamic pressure. Such lubrication is desirable for friction and wear reduction. However, in industrial applications, applied loads are often heavy and contact surfaces are rough, resulting in a breakdown of local hydrodynamic films and causing asperity interactions [1]. This lubrication regime is regarded as mixed EHL.

In a typical mixed EHL condition [2,3], the applied load is shared between the hydrodynamic pressure and asperity interaction pressure. Numerous studies have been carried out by Lubrecht, Rahnejat, Larsson et al. on a range of topics including load sharing [3,4], pressure distribution [5–7], effects of operating condition [8,9], lubricant damping [10], while numerical methods [11,12] have been developed to simulate this complex phenomenon and for friction prediction. The overall friction in mixed EHL consists of asperity interaction friction and lubricant fluid friction. The fluid friction can be derived by the rheological properties of the lubricant. However, because of the random distribution of the surface profiles, the asperity interaction in mixed EHL often have very different local contact conditions (elastic/plastic deformation, boundary film lubrication, solid-to-solid interaction, etc.), which results in different contact and/or lubrication mechanisms. As a result, the prediction of the asperity interaction friction in mixed EHL remains difficult [13].

Studies on mixed EHL friction generally consider that the frictional behaviour of the asperity interaction involves a thin layer of boundary film [13–15] in between the contacted asperities, often in a magnitude of nano-meters. The frictional behaviour of such boundary film is determined by the shear flow property of the boundary film, which is independent from the bulk fluid viscosity and is a function of the physico-chemical property of the lubricant and loading conditions [16]. Because of the random distribution of the asperities, elastic and plastic interactions continuously occur during the sliding process. It's also found that, under high local pressure, the boundary film may break down and cause solid-to-solid contact, where the friction coefficient is determined by the mechanical interaction of the asperities [17]. As a result, the frictional behaviour of the asperity interaction results from combined effects of the rheological property of the boundary film and the deformation process of the asperities. To predict the friction of asperity interactions in mixed EHL, the following topics that need to be further studied are:

1) prediction of the boundary film friction,
2) determination of the loading condition when the local boundary film breaks down, and
3) prediction of the solid-to-solid contact friction where the boundary film breaks down.

* Corresponding author.
E-mail address: xiaogang.zhang@unsw.edu.au (X. Zhang).

http://dx.doi.org/10.1016/j.triboint.2017.04.032
Received 11 December 2016; Received in revised form 14 April 2017; Accepted 20 April 2017
Available online 22 April 2017
0301-679X/

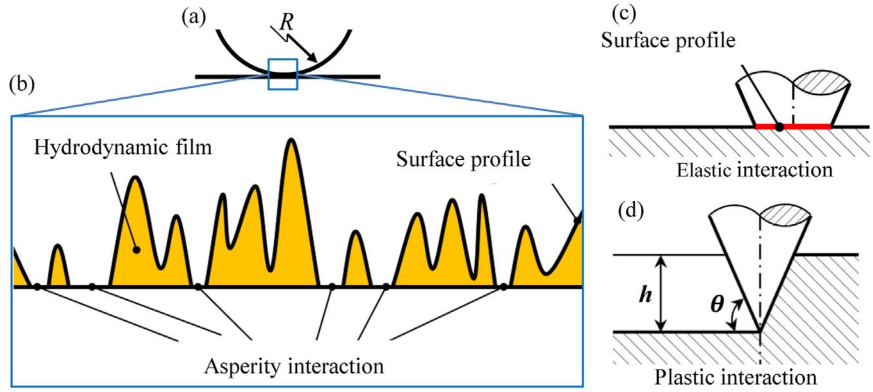

Fig. 1. The friction mechanisms in mixed EHL. (a) A perfectly flat surface in contact with a rough surface with a radius of curvature of R, (b) possible contact mechanisms at a high resolution, (c) illustration of an elastic interaction separated by a thin boundary film, (d) illustration of a plastic interaction caused by a high asperity ploughing the counter surface.

Although there are numerous researches on the frictional and mechanical behaviours of boundary film and boundary lubrication, some questions, in particularly for the prospective of friction prediction *in mixed EHL*, need further investigation. Up to date, to the authors' knowledge, there is no numerical model available in literature for the prediction of the friction coefficient of asperity interactions in mixed EHL.

Existing friction prediction methods often use an experimentally measured friction coefficient in boundary lubrication. For examples, Rahnejat et al. [3], Martini et al. [13], Khonsari et al. [18], Zhu et al. [19,20], Li et al. [21,22], and Chang et al. [23] used an experimentally obtained constant friction coefficient in boundary lubrication to approximate the asperity interaction friction coefficient, and then the overall friction coefficients of mixed EHL were predicted. Those predictions demonstrated good agreements with experimental results. However, this experimental approach may be time consuming and sometimes impractical. For example, for a given rolling-sliding contact, the friction coefficients in boundary lubrication can be different in various operating conditions (i.e., surface topography, load, etc.) [24–27], so experiments have to be conducted in these specific operating conditions. Consequently, there is a need to develop an alternative, cost-effective method to estimate the friction in mixed EHL.

Komvopoulos et al. [28–30] reports a series of observations on the frictional behaviour of boundary lubrication. Those observations reveal two kinds of behaviours of the asperity interactions. When the boundary film is not disrupted, the primary deformation mode of an asperity is in elastic, and the contribution of asperity deformation to the overall friction is negligible. In such condition, the shearing of the boundary film predominates the frictional behaviour [28]. When the local boundary film breaks down due to high pressure, direct solid-to-solid contact takes place. It is observed that the breakdown of the local boundary film often involves plastic deformation, ploughing and interfacial adhesion, which results in surface damage and high friction coefficient [28]. Consequently, the friction of asperity interaction is the combination result of the shear flow property of the lubricants and the solid-to-solid interaction of asperities. Finally, the asperity interaction friction can be predicted from either the boundary film friction or solid-to-solid ploughing and adhesion friction depending on the local contact and deformation conditions. By applying their work published in [29], the asperity interaction friction in mixed EHL can be predicted.

In this study, a numerical approach was developed based on the boundary friction theory by Komvopoulos et al. [28–30] to predict the friction coefficient in mixed EHL. The lubrication and contact condition was calculated by using a mixed EHL model, where the hydrodynamic lubrication and asperity interaction regions, as well as the hydrodynamic and asperity interaction pressure distributions were determined. Then the friction coefficient was predicted by the weighted sum of the hydrodynamic friction and asperity interaction friction. In particular, the asperity interaction friction was considered to be the combination results of the shear flow properties of boundary film and solid-to-solid ploughing and adhesion effects. The boundary film friction was predicted based on the boundary film properties, and the solid-to-solid contact friction was predicted by the local contact geometry, load, deformation, and material properties. Theoretical background and numerical procedures of mixed EHL friction prediction are presented in Section 2. To validate the numerical approach, predictions were compared with experimental results. Detailed validation is presented in Section 3. In Section 4, the numerical approach was used to investigate the frictional behaviour and role of key factors in typical operating conditions. In particular, the friction mechanisms of rolling-sliding contact in mixed EHL were studied by investigating the interactions of the fluid, boundary film and solid-to-solid components of friction. Section 5 summarizes the key outcomes and future work.

2. The friction prediction of rolling sliding contact in mixed EHL

2.1. The mechanisms of the mixed EHL friction

The friction in mixed EHL arises from the lubricant friction and asperity interaction friction where local film breaks down. The friction mechanisms of a typical rolling-sliding contact in mixed EHL are illustrated in Fig. 1. The applied load is supported by the hydrodynamic and asperity interaction pressure. The nominal contact region consists of the hydrodynamic region and the asperity interaction region. The overall friction coefficient is the sum of the lubricant fluid and asperity interaction friction coefficients.

For the friction prediction of rolling-sliding contact in mixed EHL, several assumptions were adopted in this approach.

1) A 2D (two-dimensional) simplification was adopted, as it is appropriate to develop a 2D nominal line contact (plane strain) configuration for the contact of real engineering profiles.
2) The asperity interaction was considered to have two different frictional behaviours depending on the loading and deformation of local asperities. When the local asperity is in elastic deformation, the asperity interaction friction is predominated by the rheological properties of the boundary film, and the contribution of the asperity elastic deformation to friction is negligible. The breakdown of the boundary film often involves plastic deformation of asperities, where the asperity interaction friction is predominated by the solid-to-solid interaction of asperities. In such condition, the main friction mechanisms are the ploughing and adhesion effects.
3) In reality, solid-to-solid ploughing and adhesion interaction is often generated from not only asperities, but also wear debris. In the current study, solid-to-solid friction is assumed to be contributed

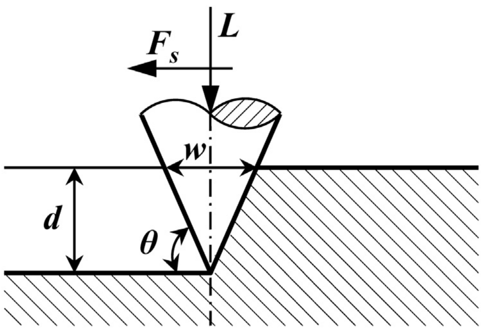

Fig. 2. Solid-to-solid friction of a conical asperity by ploughing and adhesion effects.

only by asperities while the influence of wear particles was neglected.

Assumption 1 is reasonable for gears, rolling-element bearings, and cams where the surface finish is generally consistent with the requirements of the 2D simplification [31–33]. Assumption 2 is based on the experimental observation by Komvopoulos [28,29]. Assumption 3 was adopted to simplify the friction prediction, because the mechanisms of the generating, moving, and interacting of wear debris are very complicated, which is beyond the scope of the current manuscript. Consequently, the overall friction F was calculated by the lubricant fluid, boundary film, and solid-to-solid frictions as given in Eq. (1).

$$F = F_h + F_b + F_s \tag{1}$$

where F is the overall friction of rolling-sliding contact in mixed EHL, F_h is the lubricant fluid friction in the hydrodynamic region, F_b is the boundary film friction where local boundary film is not disrupted, and F_s is the solid-to-solid friction where local boundary film is disrupted.

The overall friction coefficient μ of a rolling sliding contact in mixed EHL was obtained by Eq. (2).

$$\mu = \frac{F_h + F_b + F_s}{w} \tag{2}$$

where w is the applied load.

2.2. The lubricant fluid friction F_h

The lubrication and contact condition was studied by solving the widely used mixed EHL model by Hu et al. and Zhu et al. [34]. This model is capable of calculating the measured surface topographies under different operating conditions (i.e. load, velocity, surface roughness, slide-to-roll ratio). By using this model, the hydrodynamic region, the asperity interaction region, the hydrodynamic pressure distribution, the asperity interaction pressure distribution and the film thickness distribution were determined. The mixed EHL model is governed by several equations, the Reynolds equation, the film thickness equation, lubricant properties equations, the load balance equation, etc. The solution procedures can be easily found in literature [34]. By solving this mixed EHL model, the contact and lubrication condition of mixed EHL were obtained and illustrated in Fig. 1. Then the lubricant fluid friction F_h was predicted by the integration of the shear stress, as given in Eq. (3) [35].

$$F_h = \int \tau_f \,\mathrm{dx} \tag{3}$$

where τ_f is the lubricant shear stress.

2.3. The boundary friction F_b

Numerous measurements were conducted by researchers on the frictional behaviour of boundary film. Briscoe and Smith [36,37] investigated the shear properties of thin organic polymeric films and found that the shear stress τ_b has a linear relationship with the contact pressure, as expressed by Eq. (4).

$$\tau_b = \tau_0 + \alpha p \tag{4}$$

where τ_b is the shear stress of the boundary film, τ_0 is the shear stress of the boundary film at zero pressure, α is the interfacial shear stress–pressure coefficient, and p is the pressure.

Such linear relationship has been validated by molecular dynamics simulations [38,39] and showed good agreement with experimental results [40]. A typical coefficient of determination of linear regression on the linear dependence of boundary film reported by Yamamoto et al. [41] is 0.992 for automatic transmission fluids. In this study, Eq. (4) was used to determine the friction of boundary film. The overall boundary film friction was calculated by the integration of the shear stress, as shown in Eq. (5).

$$F_b = \int \tau_b \,\mathrm{dx} = \int (\tau_0 + \alpha p)\,\mathrm{dx} \tag{5}$$

2.4. The solid-to-solid interaction friction F_s

The breakdown of the boundary film often involves plastic deformation of asperities, where the friction is predominated by the solid-to-solid ploughing and adhesion effects. However, the geometry of an asperity can be random. Theoretical calculations for the ploughing and adhesion effects are often based on simplifications. Simple shapes as cones, spheres and pyramids are often used by investigators and their calculations agree with the experimental results fairly close. Therefore, a contact model of conical asperity was adopted in the current study, as shown in Fig. 2. The friction force derived by Komvopoulos [28,29], as given in Eq. (6), was employed to predict the asperity interaction friction in plastic contact.

$$F_s = \frac{w^2}{4}\sigma\left[\tan\theta + \left(\frac{s}{\sigma}\right)\sec\theta\right] \tag{6}$$

Where F_s is the asperity interaction friction in plastic contact, σ and s are the yield and shear strengths, and θ is calculated by the contact width w and the depth of penetration d.

In the current study, the asperity interaction friction was derived either from the properties of the boundary film or the mechanical interactions of asperities depending on the local contact conditions. The overall friction in mixed EHL was then predicted as the combination results of the lubricant fluid, boundary film, and solid-to-solid ploughing and adhesion frictions. This numerical approach was then used to study the frictional behaviour and investigate friction mechanisms of rolling-sliding contact in mixed EHL.

3. Validation of the friction prediction model

To validate the friction prediction model, the numerical results were compared with experimental results in mixed EHL under same loading conditions. Recent experimental results by Khonsari et al. [14] obtained on a twin discs machine were used for the comparison. Experimental work suggests that actual surface distributions are rather close to Gaussian [42], so Gaussian distribution is widely used to approximate a rough surface when measurement is not available [43]. Surface profiles in the calculations were numerically generated Gaussian surface profiles where their surface roughness values (Rq) are 0.283 and 0.465 μm respectively. The loading and test rig parameters are listed in Table 1. The solution domain was set to be $-4.5 \le x/b \le 1.5$ by considering that the inlet generally has important influence on the lubrication, where x is the coordinate in the rolling/sliding direction and b is the half width of Hertzian contact. The solution domain was set to a unified grid where the node number is 2000, corresponding to a dimensionless mesh size of $\Delta x/b = 0.004$, which is smaller than the typical mesh size of 0.0117 reported by Zhu et al. [44]. The convergence criterion is $\varepsilon = \sum |P^{new} - P^{old}| / \sum P^{new} < 0.0001$, which is widely used in lubrication analysis [20,45]. The boundary film parameters τ_0 and β are lubricant specific constants determined by the properties of the lubricant and

Table 1
Loading and material property parameters for mixed EHL validation.

Parameters	Values	Parameters	Values
Dimensionless Load $W=\frac{w}{E'r}$	$1\times10^{-4}/4\times10^{-5}$	Slide-to-roll ratio S	0–1
Dimensionless rolling velocity $U_r=\frac{\eta_0 U}{E'r}$	1×10^{-11}	Equivalent radius r	0.0221 m
Reference density of lubricant ρ_0	888 kg/m^3	Surface roughness σ	0.283/ 0.465 μm
Thermal conductivity of lubricant k_f	0.145 W/mK	Reference viscosity η_0	0.35 Pa s
Thermal conductivities of rollers k_a, k_b	47 W/mK	Ambient temperature T_0	293.15 K
Specific heats of rollers c_a, c_b	460 J/Kg K	Densities of rollers ρ_a, ρ_b	7850 kg/m^3
Equivalent elastic modulus E'	2.28×10^{11} Pa		

contact surfaces [36,37]. These parameters have been examined in different ways and by several researchers, where τ_0 is found in a range of 1–8 MPa and β is in a range of 0.05–0.15 [46–48]. Hence, the parameters are assumed to be τ_0=2 MPa and β=0.1 for the lubricant used in the experiments, as used in ref [49] for the boundary film friction prediction of general engine oil. The calculation of the solid-to-solid contact friction involves the determination of the yield and shear strengths. Hardness testing is often an economical substitute for most of the metals if yield strength testing is not available [50] since indentation hardness correlates linearly with yield strength [51]. In the current calculation, the yield strength was derived from the hardness, and the shear strength is 0.2 times of the yield strength [35].

Numerical results were compared with experimental results at two different loads and surface roughness values. The experimental and numerical results under the influence of slide-to-roll ratio are shown in Fig. 3, at dimensionless load $W=1\times10^{-4}$ and 4×10^{-5}, and surface roughness σ=0.283 and 0.465 μm. The numerical results predicted the same trend with experimental results. There is an increasing trend of friction coefficients when the slide-to-roll ratio is less than 0.2. The increase is due to Newtonian and non-Newtonian response of the lubricant where the shear stress at first is proportional to the shear rate, followed by shear thinning effects. At a slide-to-roll ratio of approximately 0.2 the shear stress may have reached the limiting shear stress, and therefore the friction coefficient does not continue to increase. Similar trend was also reported in [52] and [53]. For the dimensionless load of $=1\times10^{-4}$, there is a slightly decreasing trend when the slide-to-roll ratio is larger than 0.6. This is because when the slide-to-roll ratio keeps increasing, large sliding velocity would induce a significant temperature increase which causes a decrease in the viscosity of the lubricant, resulting in a decrease in the friction coefficients [14]. For the dimensionless load of 4×10^{-5}, the friction coefficients also decreased when the slide-to-roll ratio was larger than 0.6, but the decreasing rate was not as obvious as that of the dimensionless load 1×10^{-4}. This is because, for the same surface roughness and entrainment velocity, larger load would generate higher temperature, resulting in a decrease in viscosity and friction coefficient.

The main discrepancy between the numerical and experimental results lies in the absolute values of the friction coefficients. The error between the numerical and experimental results is about 10%. A possible reason for this may be the difference in surface profiles in experiments and numerical calculations, despite the surface roughness values (Rq) are the same. The current numerical analysis results are in a good agreement with the experimental data, so the numerical approach has proven to be reliable to predict friction coefficient of rolling-sliding contact in mixed EHL.

4. Results and discussions

The friction of mixed EHL is determined by considering hydrodynamic friction, boundary film friction, and solid-to-solid friction. This model provides a tool to have a better understanding of the frictional behaviour and mechanisms of rolling sliding contact by investigating (a) effects of rolling velocity and (b) the interaction of the three friction components and their contributions to the overall friction.

4.1. The frictional behaviour of rolling-sliding contact

The rolling velocity has a significant influence on the hydrodynamic effects [35]. Numerical investigations were conducted to further understand the rolling velocity effects on the friction coefficient in a full range of lubrication conditions including full film, mixed and boundary lubrication. For typical gear and bearing applications in industry, the Hertzian contact pressure is often in the magnitude of GPa. The rolling velocity varies over a wide range (i.e. from 0.001 to 10 m/s). Surface finish grades, such as N4, N5, N6, and N7, are most commonly used. In such operating conditions, the rolling-sliding contact is generally in mixed EHL. In the current study, the dimensionless loads is $W=2\times10^{-4}$, which corresponds to a Hertzian pressure of 1.35 GPa. The dimensionless velocity range is 1×10^{-12}~1×10^{-8}, which corresponds to 0.001–10 m/s. The surface profile was obtained from a N4 lapping surface by using a scanning laser microscope where the obtained Rq surface roughness is 0.3 μm, as shown in Fig. 4. Loading and material property parameters are summarized in Table 2.

The friction coefficients and the lubrication condition were predicted by varying the velocity, as shown in Fig. 5. The lubrication condition evolves the negotiation of the hydrodynamic effects and the asperity interactions. It is mainly determined by the contact ratio ψ, defined as the ratio of asperity interaction pressure to the applied load. Based on Zhu's criteria [20], a contact ratio of $\psi\geq85\%$ is defined as the boundary lubrication regime, a contact ratio of $0<\psi<85\%$ is defined as the mixed EHL regime, and a contact ratio of ψ=0 is defined as the full film lubrication regime. Fig. 5 clearly demonstrates the decisive

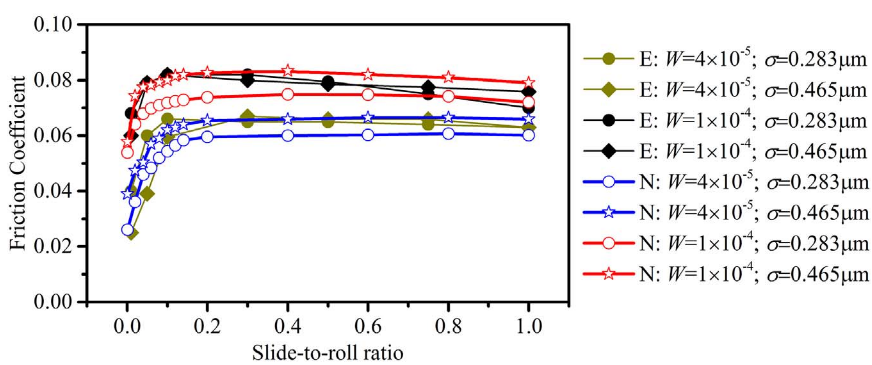

Fig. 3. Friction coefficient comparison of mixed EHL for the dimensionless load of 1×10^{-4} and 4×10^{-5} E – Experimental results, N – Numerical results.

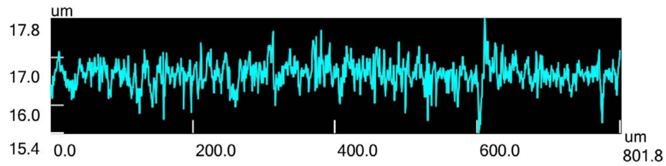

Fig. 4. N4 finish surface profile.

Table 2
Loading and material property parameters for the mixed EHL friction prediction.

Parameters	Values	Parameters	Values
Dimensionless Load $W = \frac{w}{E'r}$	2×10^{-4}	Slide-to-roll ratio S	0.25
Dimensionless rolling velocity $U_r = \frac{\eta_0 U}{E'r}$	$1\times10^{-12}\sim1\times10^{-8}$	Equivalent radius r	0.02 m
Reference density of lubricant ρ_0	888 kg/m^3	Surface roughness σ	0.30 µm
Thermal conductivity of lubricant k_f	0.145 W/mK	Reference viscosity η_0	0.2 Pa s
Thermal conductivities of rollers k_a, k_b	47 W/mK	Ambient temperature T_0	293.15 K
Specific heats of rollers c_a, c_b	460 J/Kg K	Densities of rollers ρ_a, ρ_b	7850 kg/m^3
Equivalent elastic modulus E'	2.28×10^{11} Pa		

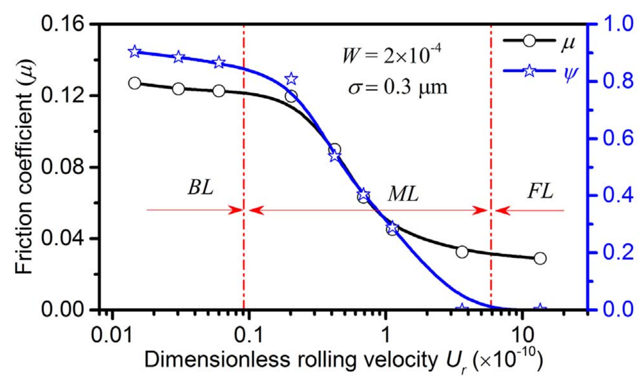

Fig. 5. Effects of the contact ratio and lubrication condition on the friction coefficient BL- boundary lubrication; ML- mixed EHL; FL-full film lubrication.

influence of lubrication regimes on the overall friction coefficients. The increase in velocity decreases the friction coefficient in different ways, depending on the loading and lubrication conditions. When the rolling velocities are small, the friction coefficient keeps almost constant. Then there is a dramatic decrease, and followed by a slightly decreasing trend of the friction coefficient with the increase in the velocity [20].

In the boundary lubrication regime, there were few hydrodynamic pressure built up and the applied load is supported by the asperity interaction pressure. The friction coefficient is mainly contributed by asperity interaction friction. Therefore the velocity has a very limited influence on the friction coefficients. With the increase in the velocity, the hydrodynamic effect is gradually building up and the lubrication regime transfers into the mixed EHL, where the overall friction is the combination results of the asperity interaction and lubricant fluid frictions. Since the lubricant fluid friction is often much smaller than that of the asperity interaction, there is a significant decrease in the friction coefficient with the increase in velocity. When the velocity is further increased, a full film regime is achieved and the overall friction is only contributed by the lubricant fluid friction. The reason for the further reduction in the overall friction coefficient is mainly attributed to the decrease in viscosity following the temperature increase caused by the increase of velocity.

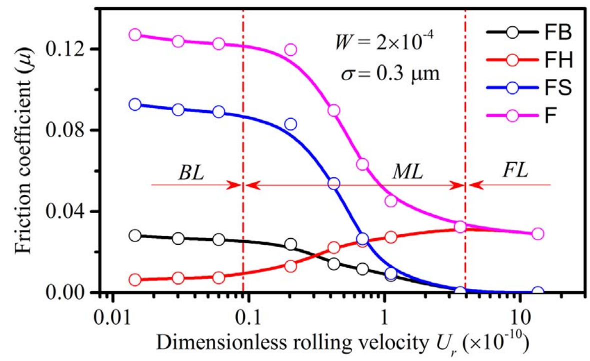

Fig. 6. Friction components of rolling sliding contact BL- boundary lubrication; ML- mixed EHL; FL-full film lubrication; F – The overall friction coefficient; FH - Lubricant fluid friction coefficient; FB - Boundary film friction coefficient; FS - Solid-to-solid friction coefficient.

4.2. The friction components and friction mechanisms

To further understand the friction mechanisms, the contributions of the three friction components to the overall friction coefficient were investigated and are presented in Fig. 6. In the boundary lubrication regime, the applied load is mainly carried by asperity interactions, and the majority are in plastic deformation. Solid-to-solid ploughing and adhesion friction, existing in the asperity contacts where the boundary film breaks down, accounts for about 75% of the overall friction. This demonstrates why in such condition friction and wear are often harsh. Also, boundary film friction, generated from the rheological properties of the boundary film in between the elastically deformed asperities, co-exists. In boundary lubrication regime, most of the asperities are in plastic deformation and only a few are in elastic deformation, so the boundary film friction is a small part, about 20%, of the overall friction. Due to the above reasons, the overall friction coefficient in the boundary lubrication is high and decreases very slightly with the increase in the rolling velocity U_r until the mixed EHL is reached at $U_r = 0.09\times10^{-10}$.

In mixed EHL, with the increasing of the velocity and the hydrodynamic pressure, the boundary film regions transfer into hydrodynamic region [20], which results in a continuing increase in the lubricant fluid friction. Also, some of the solid-to-solid regions transfer into boundary film regions, so the boundary film friction demonstrates a slightly decreasing trend in mixed EHL. The increase in the rolling velocity would also induce a transition of the solid-to-solid regions into boundary film or hydrodynamic regions. Due to the fact that lubricant fluid friction coefficient is much smaller than that of the solid-to-solid interaction, there is a dramatic decreasing trend of the overall friction coefficient in mixed EHL with the increase in velocity [54]. As shown in Fig. 6, the proportion of the solid-to-solid friction decreased from about 70–0% in mixed EHL with the increase in the rolling velocity. At about $U_r=4.0\times10^{-10}$, both solid-to-solid friction and boundary film friction decrease to zero and the lubrication regime transfers into full film lubrication.

In full film lubrication, the applied load is supported by the lubricant hydrodynamic pressure, and the overall friction is all contributed by lubricant fluid friction. The lubricant fluid friction is generated from the shear resistance of lubricant [35], and demonstrates a slightly decreasing trend with the increase in velocity because of temperature and non-Newtonian effects [35].

In summary, the developed model enables us to have better understanding of the frictional behaviour and mechanism of rolling-sliding contact in mixed EHL which largely depends on the contact and lubrication conditions. The friction is dominated by the solid-to-solid ploughing and adhesion friction in boundary lubrication regime. In the mixed EHL regime, with the increase in velocity, the overall friction coefficient decreases mainly due to the decrease in the solid-to-solid friction. The boundary film friction does not show a significant influence on the overall friction in both boundary and mixed lubrication regimes.

5. Conclusions

A numerical approach was developed to investigate the frictional behaviour and the friction mechanisms of rolling-sliding contact in mixed EHL. The friction of asperity interactions was considered to be predominated by the boundary film friction or the solid-to-solid ploughing and adhesion friction depending on local contact and deformation conditions. The overall friction was predicted by the combination results of the lubricant fluid friction, boundary film friction, and the solid-to-solid friction. The model facilitates the understanding of the effects of rolling velocity on the three components of friction, and their contributions to the overall friction coefficient. The numerical results demonstrate that:

1) the friction is dominated by the solid-to-solid ploughing and adhesion friction in boundary lubrication regime (i.e. accounts for about 75% of the overall friction in the current case),
2) in the mixed EHL regime, the overall friction coefficient shows a significant decreasing trend with the increase in velocity due to the decrease in solid-to-solid friction, and
3) the boundary film friction does not show a significant influence on the overall friction in both boundary and mixed lubrication regimes (i.e. accounts for less than 20% of the total friction in both boundary lubrication and mixed EHL regimes).

This development has provided an alternative and cost effective method to estimate friction coefficient at a given surface profile and load condition. In reality, friction is a dynamic process, and the contacted surfaces are always changing due to wear. Further work will be carried out to predict frictional behaviour with considering the evolution of the surface topography, which can be achieved by applying a wear model into the current friction prediction model. For the prospective of industrial application of the current method, future work will consider prediction errors induced by experimental measurements of surface profiles and other key operating conditions.

Acknowledgement

The authors acknowledge the financial support of Australian Research Council (DP160103501) to this project.

References

[1] Bhushan B. Modern tribology handbook. CRC press; 2010.
[2] Morris N, Rahmani R, Rahnejat H, King P, Fitzsimons B. Tribology of piston compression ring conjunction under transient thermal mixed regime of lubrication. Tribol Int 2013;59:248–58.
[3] Styles G, Rahmani R, Rahnejat H, Fitzsimons B. In-cycle and life-time friction transience in piston ring–liner conjunction under mixed regime of lubrication. Int J Eng Res 2014;15:862–76.
[4] Shahmohamadi H, Rahmani R, Rahnejat H, Garner CP, King P. Thermo-mixed hydrodynamics of piston compression ring conjunction. Tribol Lett 2013;51:323–40.
[5] Rahmani R, Theodossiades S, Rahnejat H, Fitzsimons B. Transient elastohydrodynamic lubrication of rough new or worn piston compression ring conjunction with an out-of-round cylinder bore. Proc Inst Mech Eng J: J Eng Tribol 2012;226:284–305.
[6] Sahlin F, Larsson R, Marklund P, Almqvist A, Lugt PM. A mixed lubrication model incorporating measured surface topography. Part 2: roughness treatment, model validation, and simulation. Proc Inst Mech Eng J: J Eng Tribol 2010;224:353–65.
[7] Sahlin F, Larsson R, Almqvist A, Lugt PM, Marklund P. A mixed lubrication model incorporating measured surface topography. Part 1: theory of flow factors. Proc Inst Mech Eng J: J Eng Tribol 2010;224:335–51.
[8] Morris N, Rahmani R, Rahnejat H, King P, Fitzsimons B. The influence of piston ring geometry and topography on friction. Proc Inst Mech Eng J: J Eng Tribol 2013;227:141–53.
[9] Morris N, Leighton M, De la Cruz M, Rahmani R, Rahnejat H, Howell-Smith S. Combined numerical and experimental investigation of the micro-hydrodynamics of chevron-based textured patterns influencing conjunctional friction of sliding contacts. Proc Inst Mech Eng J: J Eng Tribol 2015;229:316–35.
[10] Ankouni M, Lubrecht A, Velex P. Modelling of damping in lubricated line contacts–Applications to spur gear dynamic simulations. Proc Inst Mech Eng C: J Mech Eng Sci 2016;230:1222–32.
[11] Venner CH, Lubrecht AA. Multi-level methods in lubrication. Elsevier; 2000.
[12] Venner C, Lubrecht A. Multigrid techniques: a fast and efficient method for the numerical simulation of elastohydrodynamically lubricated point contact problems. Proc Inst Mech Eng J: J Eng Tribol 2000;214:43–62.
[13] Martini A, Zhu D, Wang Q. Friction reduction in mixed lubrication. Tribol Lett 2007;28:139–47.
[14] Masjedi M, Khonsari MM. Theoretical and experimental investigation of traction coefficient in line-contact EHL of rough surfaces. Tribol Int 2014;70:179–89.
[15] Liu Z, Gangopadhyay A. Friction reduction in lubricated rough contacts: numerical and experimental studies. J Tribol 2015;138:021506.
[16] Hsu SM. Boundary lubrication: current understanding. Tribol Lett 1997;3:1–11.
[17] Bowden FP, Tabor D. The Friction and Lubrication of Solids; 1950.
[18] Lu X, Khonsari M, Gelinck E. The Stribeck curve: experimental results and theoretical prediction. J Tribol 2006;128:789–94.
[19] Zhu D, Wang QJ. On the λ ratio range of mixed lubrication. Proc Inst Mech Eng J: J Eng Tribol 2012;226:1010–22.
[20] Zhu D, Wang J, Wang QJ. On the stribeck curves for lubricated counterformal contacts of rough surfaces. J Tribol 2015;137:021501.
[21] Li S. Lubrication and contact fatigue models for roller and gear contacts. Ohio State University; 2009.
[22] Li S, Kahraman A. A method to derive friction and rolling power loss formulae for mixed elastohydrodynamic lubrication. J Adv Mech Des Syst Manuf 2011;5:252–63.
[23] Chang L, Jeng Y-R. A mathematical model for the mixed lubrication of non-conformable contacts with asperity friction, plastic deformation, flash temperature, and tribo-chemistry. J Tribol 2014;136:022301.
[24] Ponte DC, Meyer DML. Frictional behavior and topography of porous polyurethane on copper and silicon dioxide articulating contacts. J Tribol 2016:138.
[25] Spijker P, Anciaux G, Molinari J-F. Relations between roughness, temperature and dry sliding friction at the atomic scale. Tribol Int 2013;59:222–9.
[26] Xu MJ, Li L, Wang MZ, Luo B. Effects of surface roughness and wood grain on the friction coefficient of wooden materials for wood-wood frictional pair. Tribol Trans 2014;57:871–8.
[27] Tian SF, Jiang LT, Guo Q, Wu GH. Effect of surface roughness on tribological properties of TiB2/Al composites. Mater Des 2014;53:129–36.
[28] Komvopoulos K. Sliding friction mechanisms of boundary-lubricated layered surfaces: part I—basic mechanical aspects and experimental results. Tribol Trans 1991;34:266–80.
[29] Komvopoulos K. Sliding friction mechanisms of boundary-lubricated layered surfaces: part II—Theoretical analysis. Tribol Trans 1991;34:281–91.
[30] Komvopoulos K, Saka N, Suh N. The mechanism of friction in boundary lubrication. J Tribol 1985;107:452–62.
[31] Bryant MJ, Evans HP, Snidle RW. Plastic deformation in rough surface line contacts—a finite element study. Tribol Int 2012;46:269–78.
[32] Scaraggi M, Putignano C, Carbone G. Elastic contact of rough surfaces: a simple criterion to make 2D isotropic roughness equivalent to 1D one. Wear 2013;297:811–7.
[33] Rapetto MP, Almqvist A, Larsson R, Lugt PM. On the influence of surface roughness on real area of contact in normal, dry, friction free, rough contact by using a neural network. Wear 2009;266:592–5.
[34] Zhu D, Hu Y-Z. A computer program package for the prediction of EHL and mixed lubrication characteristics, friction, subsurface stresses and flash temperatures based on measured 3-D surface roughness. Tribol Trans 2001;44:383–90.
[35] Wen S, Huang P. Principles of tribology. Wiley. com; 2012.
[36] Briscoe B, Evans D. The shear properties of Langmuir-Blodgett layers. Proc R Soc Lond A: Math Phys Eng Sci: R Soc 1982:389–407.
[37] Briscoe B, Smith A. The effect of periodic loading on the shear strength properties of thin organic polymeric films. ASLE Trans 1980;23:232–6.
[38] Garvey M, Weinert M, Tysoe WT. On the pressure dependence of shear strengths in sliding, boundary-layer friction. Tribol Lett 2011;44:67–73.
[39] Gao H, Tysoe WT, Martini A. Identification of the shear plane during sliding of solid boundary films: potassium chloride films on iron. Tribol Lett 2016;62:1–8.
[40] Gao F, Furlong O, Kotvis PV, Tysoe W. Pressure dependence of shear strengths of thin films on metal surfaces measured in ultrahigh vacuum. Tribol Lett 2008;31:99–106.
[41] Eguchi M, Yamamoto T. Shear characteristics of a boundary film for a paper-based wet friction material: friction and real contact area measurement. Tribol Int 2005;38:327–35.
[42] Greenwood J, Tripp J. The contact of two nominally flat rough surfaces. Proc Inst Mech Eng 1970;185:625–33.
[43] Patir N. A numerical procedure for random generation of rough surfaces. Wear 1978;47:263–77.
[44] Hu Y-Z, Zhu D. A full numerical solution to the mixed lubrication in point contacts. J Tribol 2000;122:1–9.
[45] Dong HL, Hu JB, Li XY. Temperature analysis of involute gear based on mixed elastohydrodynamic lubrication theory considering tribo-dynamic behaviors. J Tribol 2014:136.
[46] Briscoe B, Scruton B, Willis F. The shear strength of thin lubricant films. Proc R Soc

Lond A: Math, Phys Eng Sci: R Soc 1973:99–114.
[47] Timsit R, Pelow C. Shear strength and tribological properties of stearic acid films—Part II: on gold-coated glass. J Tribol 1992;114:159–66.
[48] Timsit R, Pelow C. Shear strength and tribological properties of stearic acid films—Part I: on glass and aluminum-coated glass. J Tribol 1992;114:150–8.
[49] Kun L, Youbai X. The study of friction and mixed lubrication of piston ring-cylinder of engine. Trans CSICE 1995;3.
[50] Pavlina E, Van Tyne C. Correlation of yield strength and tensile strength with hardness for steels. J Mater Eng Perform 2008;17:888–93.
[51] Busby JT, Hash MC, Was GS. The relationship between hardness and yield stress in irradiated austenitic and ferritic steels. J Nucl Mater 2005;336:267–78.
[52] Bjorling M, Habchi W, Bair S, Larsson R, Marklund P. Towards the true prediction of EHL friction. Tribol Int 2013;66:19–26.
[53] Habchi W, Bair S, Vergne P. On friction regimes in quantitative elastohydrodynamics. Tribol Int 2013;58:107–17.
[54] Huang P. Numerical calculation of lubrication: methods and programs. John Wiley & Sons; 2013.